Effects of transient depolarizing potentials on the firing rate of cat neocortical neurons

A. D. Reyes and E. E. Fetz

J Neurophysiol 69:1673-1683, 1993.

You might find this additional info useful...

Effects of Transient Depolarizing Potentials on the Firing Rate of Cat Neocortical Neurons

ALEX D. REYES AND EBERHARD E. FETZ
Department of Physiology and Biophysics and Regional Primate Research Center, University of Washington, Seattle, Washington 98195

SUMMARY AND CONCLUSIONS

1. The effects of excitatory postsynaptic potentials (EPSPs) on interspike intervals (ISIs) of neocortical neurons can be mimicked by pulse potentials (PPs) produced by current injection. The present report documents the dependence of the ISI shortening on the amplitudes of PPs and EPSPs and on the firing rate of the affected neuron.

2. In rhythmically firing neocortical neurons, the ISI shortenings caused by PPs arriving at specific times in the ISI can be described by a shortening-delay (S-D) curve. The S-D curve yields three measures of the PPs' ability to shorten the ISI: *1*) the mean ISI shortening, S; *2*) the maximum shortening, S_{max}; and *3*) the effective interval, defined as the portion of the ISI in which the PP consistently shortens the ISI. For PPs ranging between 80 μV and 3.6 mV (and cells firing at 25 imp/s), the mean shortening increased with amplitude h as S (ms) $= 1.2 * h$ (mV)$^{1.24}$ ($r = 0.94$; $P < 0.01$). S_{max} increased linearly with amplitude as 4.9 ms/mV ($r = 0.86$, $P < 0.01$). The effective interval (as a percentage of the ISI) increased slightly with PP amplitude and had a mean value of $65 \pm 21\%$ (mean $\pm$ SD).

3. S-D curves obtained with stimulus-evoked EPSPs varied with EPSP amplitude in a manner similar to those of PPs. The relations obtained for stimulus-evoked EPSPs were not statistically different from those obtained for PPs in the same cells.

4. To determine the effect of firing rate, PPs were applied while neurons fired at frequencies ranging from 8 to 71 imp/s. Both S and S_{max} were approximately inversely proportional to the baseline firing rate (f_o) and could be described as: S or $S_{max} - kf_o^{-m}$. The mean value of the exponent m ($\pm$SD) was 0.96 ± 0.25 for S and 1.2 ± 0.4 for S_{max}. These values were not statistically different from a value of 1 (1 group, 2-tailed t test). The effective interval did not vary significantly with firing rate.

5. The dependence of S on PP amplitude and baseline firing rate was incorporated into an expression for the average change in firing rate (Δf) produced by PPs occurring at rate f_s: $\Delta f - 0.03 h^{1.24} f_s$. The Δf increased with PP amplitude but did not vary significantly with the baseline firing rate. The values of Δf calculated from the S-D curves matched the values that were computed directly from the spike trains.

6. Comparison of Δf produced by brief pulses of current with Δf produced by the same net increment in current applied steadily revealed that the pulses produced significantly larger increases in the firing rate. Thus synaptic inputs arriving synchronously as transient pulses have a greater effect on the firing rate of cortical neurons than the same inputs arriving asynchronously.

INTRODUCTION

The quantitative effects of synaptic potentials on activity of cortical neurons remains a fundamental concern in understanding the functional consequences of synaptic inter-actions between neurons (e.g., Abeles 1991; Douglas and Martin 1990). Intracellular records of cortical neurons obtained from in vivo preparations reveal synaptic potentials with complex waveforms, as evoked during visual stimulation (Creutzfeldt et al. 1974; Ferster 1986; Jagadeesh et al. 1992) and during active movements (Chen and Fetz 1991; Matsumura 1979). The functional consequences of such fluctuating synaptic input may not be predictable from plots of firing frequency versus steady mean current.

The companion paper (Reyes and Fetz 1993) showed that transient depolarizing pulse potentials (PPs) obtained by injecting brief current pulses could shorten the interspike intervals (ISIs) by two mechanisms: a time-varying firing level allowed the PPs near the end of the ISI to cross threshold directly, and a slow regenerative process allowed earlier PPs to shorten the ISI through delayed crossings. The ISI shortenings caused by PPs were found to mimic those produced by comparable evoked excitatory postsynaptic potentials (EPSPs). In this report, we document the effect of the amplitude of depolarizing potentials and the baseline firing rate of the cell on the ISI shortenings. These relations are incorporated into a general expression for the change in firing rate (Δf) produced by transient depolarizing potentials. Finally, we show that the increase in firing rate evoked by repetitive PPs or EPSPs will exceed that produced by the same increment of steadily applied current.

METHODS

Intracellular recordings were made from layer V neocortical neurons in slices of the cat sensorimotor cortex. Experimental procedures and data analysis are described in the preceding paper (Reyes and Fetz 1993). To approximate EPSPs, we injected brief depolarizing current pulses (amplitude, 0.1–4.0 nA; duration, 0.5–2 ms) through the electrode, producing transient depolarizing PPs (e.g., Fig. 2, *left*). These PPs were evoked repetitively and randomly in cells that were induced to discharge regularly by a steadily injected current. The firing rate was monitored continually on an oscilloscope, and the current was adjusted if the firing rate deviated from the desired target rate.

The ISI shortenings caused by PPs at specific times in the ISI were described by a shortening-delay (S-D) curve (see Fig. 1 of Reyes and Fetz 1993). PP delay was the time from the initial spike of the ISI to the onset of the PP and is expressed as a percentage of the preceding control ISI. The duration of the shortened ISI was subtracted from the control ISI to determine the shortening produced by the PP. Over many trials, the mean shortening and the variance (both given as percentage of the control ISI) were calculated for each delay and plotted on the S-D curve. Three parame-
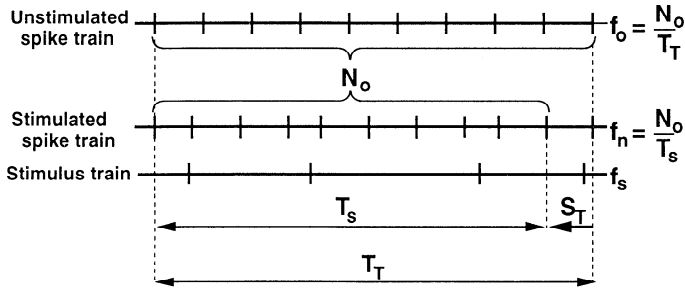
FIG. 1. Parameters for calculating net Δf produced by transient depolarizing pulse potentials (PPs). *Top trace* represents train of spikes at rate f_0 in absence of stimuli. *Middle trace* shows train of spikes at f_n during stimulation, and *bottom trace* shows the PP stimulus train at rate f_s. N_0 is number of spikes that occurred over the total time interval, T_T, in the unstimulated train and over T_s during stimulation. The difference between T_T and T_s is the total shortening, S_T, caused by the PPs.

ters were measured from the S-D curve: the mean shortening, S; maximum shortening, S_{max}; and the effective interval, defined as the portion of the ISI during which the PP consistently shortened the ISI.

Increase in firing rate caused by PPs

The Δf produced by the PPs in a repetitively discharging neuron can be calculated from the S-D curves. If we assume that the PP is introduced no more than once in any given ISI and that the PP affects only the interval in which it occurs, the mean amplitude of the S-D curve gives the mean shortening of randomly occurring PPs.

The net Δf produced by randomly occurring PPs can be derived from the spike trains as follows (see Fig. 1). If the unstimulated cell fires at a rate f_0 (*top trace*), the number of spikes, N_0, that occur over the total time interval, T_T, is

$$N_0 = f_0 T_T \qquad (1A)$$

and

$$f_0 = N_0/T_T \quad (\text{imp/s}) \qquad (1B)$$

During stimulation (*bottom trace*), the firing rate increases by Δf to a new firing rate, f_n (*middle trace*),

$$f_n = f_0 + \Delta f \quad (\text{imp/s}) \qquad (2)$$

and N_0 spikes would occur over a shorter time period, $T_s = T_T - S_T$, where S_T is the total shortening produced by all the PPs. Thus

$$N_0 = f_n(T_T - S_T) \qquad (3A)$$

and

$$f_n = N_0/(T_T - S_T) \quad (\text{imp/s}) \qquad (3B)$$

If each PP produces a mean shortening of S, then $S_T \cong N_s S$, where N_s is the total number of stimuli (i.e., PPs) over the interval T_s. Alternatively, if f_s is the mean stimulus rate, then $N_s = f_s T_s = f_s(T_T - S_T)$ and

$$S_T = f_s(T_T - S_T)S \qquad (4)$$

Combining *Eqs. 1B, 2, 3B*, and *4* yields Δf as

$$\begin{aligned}
\Delta f &= f_n - f_0 \\
&= N_0/(T_T - S_T) - N_0/T_T \quad (\text{from } Eqs.\ 1B \text{ and } 3B) \\
&= N_0 S_T/[T_T(T_T - S_T)] \\
&= f_0 f_s S \qquad (5)
\end{aligned}$$

Thus the net Δf is equal to the product of stimulus rate, the firing rate, and the mean ISI shortening.

RESULTS

The data presented here were obtained from the same 66 neurons described in the preceding paper (Reyes and Fetz 1993).

Effects of PP amplitude on interval shortening

Figure 2 (*right*) illustrates the S-D curves obtained from one cell, firing at 25 imp/s, for PPs with amplitudes ranging from 80 μV to 1.0 mV (Fig. 2, *left*). Each PP caused measurable ISI shortenings. The effective interval ranged from 48 to 66% of the ISI and did not vary significantly with PP amplitude (*cell A6* in Table 1).

The most prominent effect of varying the PP amplitude occurred late in the ISI. The S-D curves derived from the 0.7- and 1.0-mV PP showed markedly larger shortenings than those of the smaller PPs. At delays between 84 and 100%, the PPs crossed firing level directly, triggering an action potential at short, fixed latencies; thus the ISI shortening decreased linearly with delay, and the variance of the S-D curves (*right bottom traces*) was significantly reduced. At intermediate delays (34–83%) the PPs shortened the ISIs indirectly through delayed crossings involving a slow regenerative process described in the preceding paper (Reyes and Fetz 1993). By comparison, the smaller PPs (≤ 0.3 mV) produced fewer direct crossings, as indicated by the lack of distinct decreases in the variance. [However, some direct crossings very late in the ISI may be masked by unavoidable measurement errors (see Reyes and Fetz 1993).]

The effects of PP amplitude were quantified with the use of three parameters of the S-D curve: *1*) the mean shortening, S; *2*) the peak shortening, S_{max}; and *3*) the effective interval. The mean shortening is plotted against PP amplitude in Fig. 3A ($\square$) for 48 PPs ranging in size from 80 μV to 3.6 mV. Only data from cells ($n = 28$) that were induced to fire at 25 imp/s are included in the graph. A single regression line [S (ms) $= 1.7\ h$ (mV) $- 0.3$; $R = 0.88$; $P < 0.01$] could be fit to the pooled data; however, this did not optimally describe the data points for small PPs because the intercept did not go through the origin. The relation in the total range was better fit with an exponential relation

$$S - 1.2h^{1.24} \quad (R - 0.94, P < 0.01) \qquad (6A)$$

where S is in milliseconds and h is the PP amplitude in millivolts.

Figure 3B plots the relation between PP amplitude and mean shortening for PPs <1 mV, which is more relevant to the range of unitary EPSPs. The curvilinear fit for these points is nearly identical with that obtained for the total range of PP amplitudes

$$S = 1.2h^{1.26} \quad (R = 0.93, P < 0.01) \qquad (6B)$$

S_{max} was also positively correlated with PP amplitude (Fig. 3C). A single regression line [$S_{max} = 4.9h - 1.5$] adequately described the relation ($R = 0.86$, $P < 0.01$) for the complete range.

The effective interval (Fig. 3D) increased significantly ($P < 0.01$) with PP amplitude (effective interval, 9.8%h + 57.3%), but the correlation coefficient of this fit was small
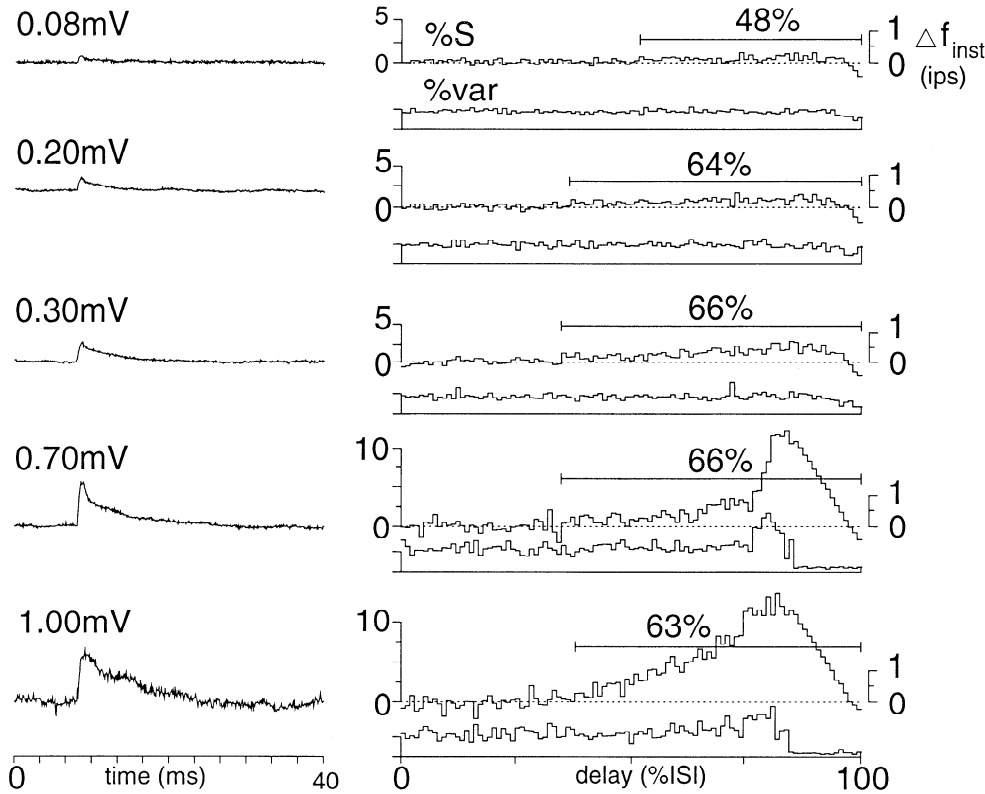
FIG. 2. Shortening-delay (S-D) curves obtained for different pulse potential (PP) amplitudes in the same cell. *Left*: PPs recorded at rest, ranging in amplitude from 0.08 to 1.00 mV. *Right*: corresponding S-D curves (*top traces*) and percentage of variance of the S-D curves (*bottom traces*). Horizontal line shows the extent of the effective intervals. Abscissa in *right column* gives the delay in the interspike interval (ISI) as a percentage of the ISI. Left ordinate gives the shortening produced as a percentage of the ISI. Right ordinate gives the corresponding instantaneous Δf.

($r = 0.39$). The mean value of the effective interval for the pooled data was $65 \pm 21\%$ (mean $\pm$ SD).

The relations between these parameters and PP amplitude were obtained for single cells in addition to the pooled data. Table 1 lists the parameters of the best curvilinear fits of S with amplitude. The mean values of the parameters for all eight cells are consistent with those of the pooled data (above). Four of these cells fired at rates <25 imp/s; there is no indication that the parameters varied systematically with firing rate. Table 1 also gives the slopes and intercepts of the regression lines describing the variation of S and S_{max} and the effective interval with amplitude for these cells. The linear relation between S and PP amplitude was significant in each of the seven cells with sufficient data points for statistical analysis (≥ 5). A positive, significant relation was also found between S_{max} and PP amplitude in six of seven

cells. The effective interval varied significantly with PP amplitude in only one of the cells with sufficient data points.

Effects of PP amplitude on interval lengthening

As noted previously (Reyes and Fetz 1993), the PPs not only shortened the ISI in which they appeared but also lengthened the subsequent ISI by a small amount. These lengthenings could be described by a modified S-D curve whose abscissa represents the delay of the PP in the preceding interval (cf. Fig. 10B, Reyes and Fetz 1993). The mean lengthenings of the succeeding intervals increased with PP amplitude, as illustrated in Fig. 3, A and B (diamonds). A single regression line with a slope of -0.17 ms/mV adequately described the relation ($R = 0.64$, $P < 0.01$). The curvilinear fit for the (negative) shortening of the subse-

TABLE 1. *Variation of S-D curve parameters with PP amplitude*

Amplitude Range. mV	n	Firing Rate. imp/s	$S = kh^m$			$S = ah + b$			$S_{max} = ah + b$			$EI = ah + b$		
			k	m	R	a	b	R	a	b	R	a	b	R
Cell														
A1	1.3–5.1	10	16.7	1.5	1.3	0.91*	2.5	−0.8	0.97*	6.2	−1.9	0.97*	4.3	58.3	0.41
A2	0.2–1.8	5	18.0	1.2	1.3	0.99*	1.5	−0.3	0.99*	3.3	0.4	0.92	22.7	46.2	0.83
A3	0.9–9.5	9	20.0	1.2	1.0	0.94*	0.9	0.7	0.93*	2.5	4.1	0.89*	−0.1	61.7	0.04
A4	0.1–2.6	6	18.0	1.5	1.3	0.98*	2.0	−0.2	0.98*	4.6	0.0	0.98*	16.2	46.6	0.82*
A5	0.2–0.7	7	25.0	0.7	1.4	0.73	0.7	0.0	0.87*	3.4	0.0	0.88*	52.3	31.0	0.55
A6	0.08–1.0	13	25.0	1.3	1.1	0.94*	1.8	−0.2	0.95*	8.2	−0.5	0.94*	2.2	50.2	0.22
A7	0.1–0.3	4	25.0	1.2	1.3	0.76	1.0	0.0	0.82	2.2	0.3	0.97	163.2	42.6	0.98
A8	0.1–1.0	7	25.0	0.9	1.0	0.87*	0.9	0.0	0.94*	2.5	0.2	0.92*	9.7	89.0	0.20
Mean				1.2 ± 0.3	1.2 ± 0.2	0.89 ± 0.10	1.4 ± 0.6	-0.1 ± 0.4	0.93 ± 0.06	4.1 ± 2.1	0.3 ± 1.7	0.93 ± 0.04	33.8 ± 54.9	53.2 ± 17.2	0.51 ± 0.35

Values in Mean are $\pm$SD. *Significance at $P < 0.01$ (2-tailed t test). S-D, shortening delay; PP, pulse potential.
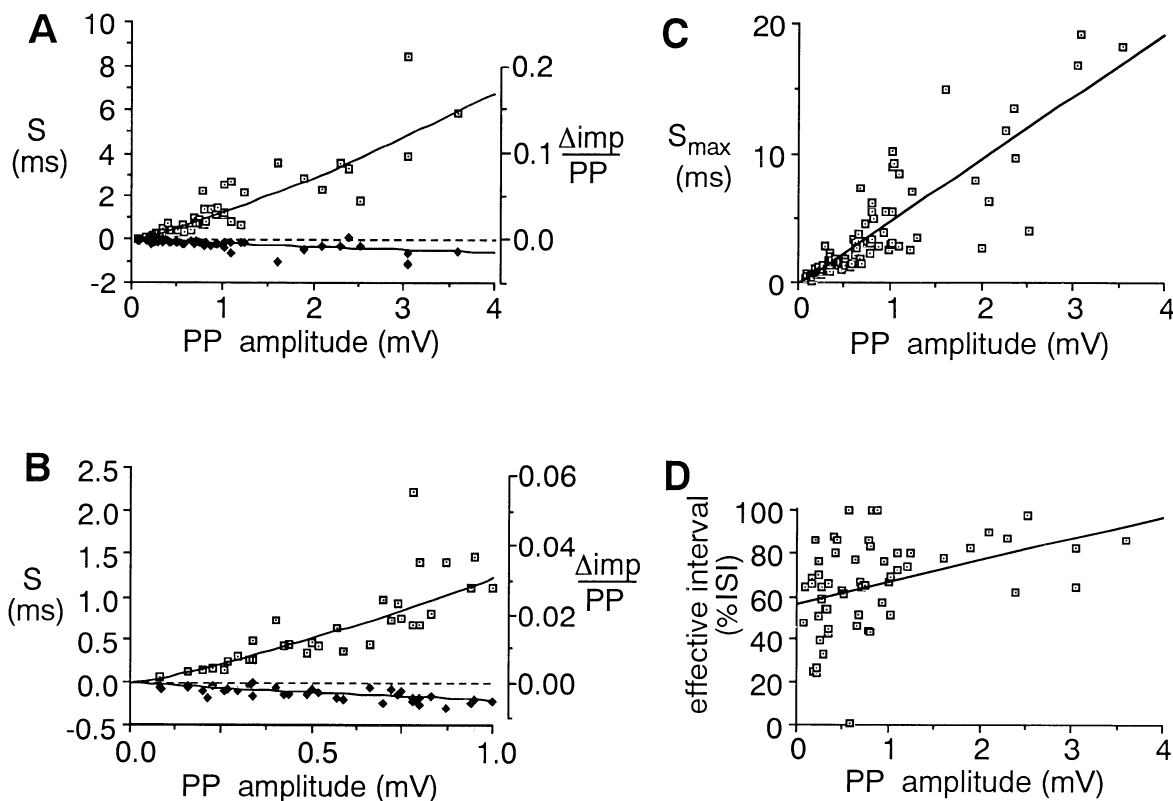
FIG. 3. Variation of shortening-delay (S-D) curve parameters with pulse potential (PP) amplitude. A: mean shortening, S, as a function of PP amplitude, h ($\square$) for cells firing at 25 imp/s. Data points could be fitted with an equation of the form $S = 1.2 * h^{1.24}$ ($R = 0.94$, $P < 0.01$). Mean Δimp/PP (right ordinate) increased with PP amplitude as $0.03\ h^{1.24}$. Filled diamonds plot lengthening of succeeding interval as function of delay in preceding interval. B: S as function of amplitude for smaller PPs, <1 mV. C: peak of the S-D curve (S_{max}) increased linearly with PP amplitude with a slope of 4.9 ms/mV ($r = 0.86$, $P < 0.01$). D: effective interval increased with PP amplitude with a slope of 9.8%/mV ($r = 0.39$, $P < 0.01$).

quent interval was S_2 (ms) = $-0.19\ h^{0.76}$ ($R = 0.77$, $P < 0.01$).

Effect of EPSP amplitude on interval shortening

As shown previously (Reyes and Fetz 1993), stimulus-evoked EPSPs shortened the ISI in a manner similar to that of PPs. To investigate the effect of EPSP amplitude on the ISI shortenings, we constructed S-D curves for EPSPs with amplitudes ranging from 0.4 to 4.4 mV. Figure $4A$ ($\bigcirc$) plots the mean shortening (S) against EPSP amplitude for 31 EPSPs (11 cells). The neurons were induced to fire at rates ranging from 16 to 20 imp/s. S increased with EPSP amplitude (h_E) as $S = 0.8\ h_E^{1.3}$ ($r = 0.70$, $P < 0.01$). The slope of the linear regression was 1.4 ms/mV ($r = 0.58$, $P < 0.01$). S_{max} (Fig. $4B$) increased at a rate of 4.6 ms/mV ($r = 0.78$, $P < 0.01$). For this sample, the effective interval (Fig. $4C$) did not vary with EPSP amplitude and had a mean value of $76.9 \pm 16.3\%$.

These relations for EPSPs were nearly identical to those obtained for PPs in the same cells. Figure 4, A–C ($\blacklozenge$) shows the variation of S, S_{max}, and effective interval with PP amplitude (h) in the same cells. S increased as $1.0\ h^{1.3}$ ($r = 0.70$, $P < 0.01$) or, with the use of linear regression, as $1.5\ h$ ($r = 0.80$, $P < 0.01$). S_{max} increased with PP amplitude as $4.4\ h$ ($r = 0.73$, $P < 0.01$). As with the EPSPs, the effective interval did not vary significantly with PP amplitude and had a mean of $69.7 \pm 14.6\%$. These relations for PPs were

not statistically different from those of the EPSPs in the same cells ($P > 0.05$, F test). This further confirms that PPs can be used to mimic the effects of EPSPs on active neurons for a range of amplitudes.

Effects of baseline firing rate on interval shortening

Figure $5A$ shows averaged records of the membrane trajectory of a neuron firing at 12.5, 24.2, and 48.7 imp/s. With increasing firing rate, the slope of the membrane trajectory increased, and the depth of the afterhyperpolarization (V_{AHP}) decreased. These changes were probably related to changes in the activation states of various ionic conductances (Stafstrom et al. 1984a), which could also affect the ISI shortenings caused by PPs. To investigate the effect of firing rate, we applied PPs with cells firing at frequencies ranging from 8 to 71 imp/s.

The height and overall shape of the S-D curve varied remarkably little with firing rate. Figure 5, B–D illustrates the S-D curves of the cell tested with a 3.6-mV PP at various firing rates. The normalized delays at which the peaks occurred and at which the variances of the S-D curves abruptly decreased (bottom traces in Fig. 5, B–D) did not change systematically with firing rate. Thus the transition from the direct to delayed crossings occurred at relative delays that were essentially independent of the firing rate.

The fact that the transition from delayed to direct crossings remained relatively unchanged indicates that the volt-
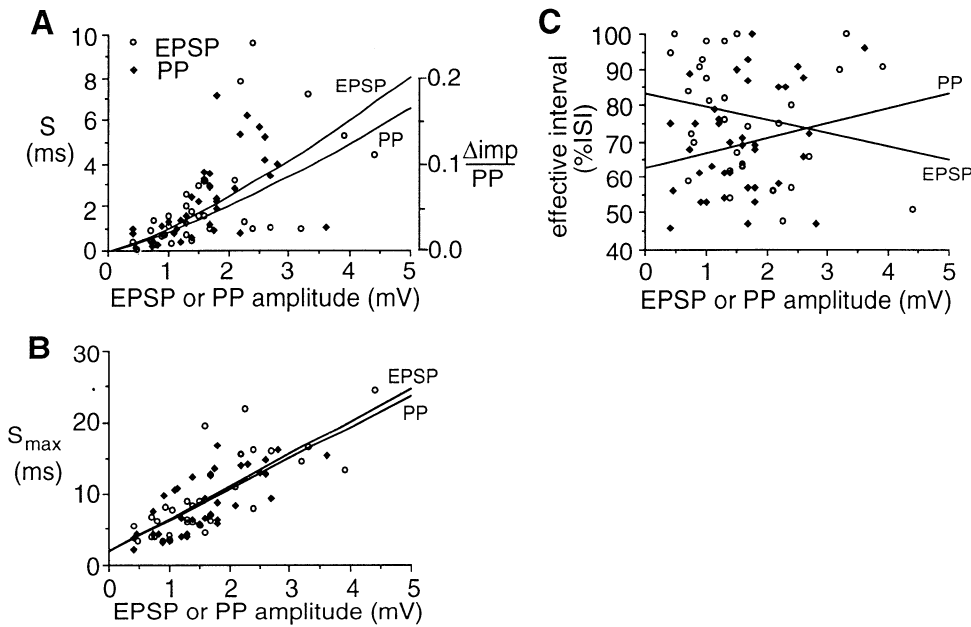
FIG. 4. Comparison of excitatory postsynaptic potentials (EPSPs) and pulse potentials (PPs): effect of amplitudes on shortening-delay curve parameters obtained from same cells. A: S increased with amplitude as $0.8\,h^{1.3}$ ($r = 0.70$, $P < 0.01$) for EPSPs ($\circ$) and as $1.0\,h^{1.3}$ for PPs ($r = 0.7$, $P < 0.01$). B: S_{max} increased as $4.6\,h$ ($r = 0.78$, $P < 0.01$) for EPSPs and $4.4\,h$ for PPs ($r = 0.73$, $P < 0.01$). C: the effective interval did not vary significantly with EPSP or PP amplitude (rising regression line corresponds to PPs).

age difference between firing level and trajectory at each normalized delay did not change with firing rate. This indicates that the time-varying firing level, like the trajectory, steepened with increasing firing rate. The oblique slashes on the trajectories in Fig. 5A represent the rising edge of the PP and are positioned at the delay where the transition occurs. The dashed curves approximate the time course of the firing level for each trajectory. Had the time course of firing level not steepened, the transition would have occurred at successively later delays in the ISI as the firing rate increased.
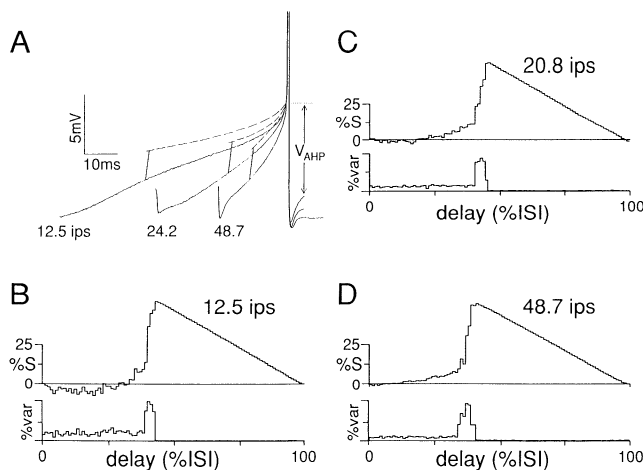

FIG. 5. Variation of shortening-delay (S-D) curve with firing rate. A: superimposed traces of averaged membrane trajectory at firing rates of 12.5, 24.2, and 48.7 imp/s. The rate of rise of the membrane trajectory increased and the depth of the afterhyperpolarization (V_{AHP}) decreased with increasing firing rate. Oblique slashes approximate the rising edge of the pulse potential (PP; amplitude, 3.6 mV) and are positioned in the interspike interval where the transition from direct to delayed crossings occurred. The estimated firing level (dashed lines) steepened with the trajectory as the firing rate increased. B–D: S-D curves obtained with a 3.6-mV PP in the same cell. There were no systematic differences between the peak heights. The variance curves (*bottom traces*) show that the delay where the transition from direct to delayed crossings occurred also did not vary systematically with firing rate.

At low firing rates, PPs appearing in the initial portion of the ISI produced a paradoxical lengthening of the ISI (Fig. 5B). These lengthenings are indicated by negative values in the S-D curves, occurring during the first 30% of the ISI. At successively higher firing rates, the initial troughs in the S-D curves became more shallow and eventually inverted at rates >20 imp/s. Such ISI lengthenings were observed in 15 of 22 cells.

Figure 6, A–C plots the variation of S, S_{max}, and the effective interval with firing rate for the cell in Fig. 5. As with most cells, S and S_{max} decreased with increasing frequency and could be described with log-log plots as

$$S(f_o) \quad or \quad S_{max}(f_o) = k f_o^{-m} \qquad (7)$$

where k is a constant. Table 2 lists the values of k and m for S and S_{max} for 11 cells (13 PPs) and includes one exception (*F12*), whose S and S_{max} increased linearly with f_o. The correlation coefficients (column 5) for the relations were generally high; in 7 of 10 cases that had 5 or more data points, the fits were statistically significant ($P < 0.01$). For S, the value of the exponent m ranged from 0.6 to 1.5, with a mean of 0.96 ± 0.25. The value of m for S_{max} ranged from 0.8 to 1.5 with a mean of 1.2 ± 0.4. Neither of these mean values was statistically different from 1 ($P > 0.05$; 1 group, 2-tailed t test). Although the effective interval tended to increase with firing rate, linear regression was statistically significant in only one cell (the cell in Fig. 6C).

The lengthening of the interval following the PP-shortened interval was most prominent at the higher firing rates. These lengthenings are plotted for the 3.6-mV PP in Fig. 6A (triangles).

Change in firing rate caused by PPs

The variation of the mean ISI shortening (S) with PP amplitude (h) and with the baseline firing rate (f_o) can be used to calculate the net change in firing rate (Δf) caused by the PPs. *Equation 5* indicates that Δf is the product of S, f_o, and the stimulus rate (f_s). Because the PPs were introduced randomly and uniformly throughout the ISI in these
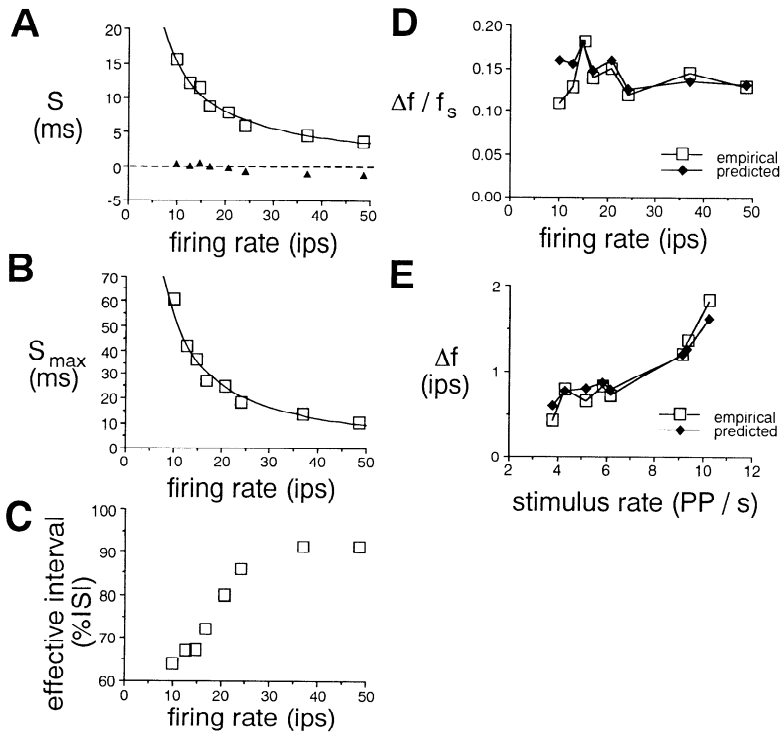
A

B

C

D

E

FIG. 6. Variation of shortening-delay (S-D) curve parameters with firing rate. Data were measured from S-D curves of Fig. 5. *A*: S decreased with firing rate as $f^{-0.9}$ ($r = 0.99$, $P < 0.01$). Filled triangles show lengthening of succeeding interval. *B*: S_{max} varied as $f^{-1.0}$ ($r = 0.99$, $P < 0.01$). *C*: effective interval as function of rate. *D*: Δf_{emp} ($\square$) and Δf ($\blacklozenge$) as a function of firing rate. Δf was normalized (divided) by the stimulus rate. *E*: Δf as a function of stimulus rate for 1 cell.

experiments, S can be obtained from the mean of the S-D curves. The baseline firing rate was taken as the average value of the reciprocals of the control ISIs that were unaffected by the PP. The stimulus rate was obtained by dividing the total number of stimuli by the total time interval. The resulting values of Δf calculated for 26 PPs ranging in amplitude from 0.4 to 3.6 mV are plotted by the striped bars in Fig. 7.

Another measure of Δf can be obtained directly from the digitized spike train. This "empirical change in firing rate,"

Δf_{emp}, is the conditioned firing rate (f_n) minus the baseline firing rate (*Eq. 2*). The conditioned rate is obtained by dividing the total number of spikes during application of the PPs by the total time interval, and baseline is again derived from the unconditioned control intervals. The solid bars in Fig. 7 plot Δf_{emp} for the same 26 PPs.

The match between the calculated and empirically measured changes in firing rate was reasonably good. The calculated values (Δf, striped bars) tended to be slightly greater than the empirical values (Δf_{emp}, solid bars), probably be-

TABLE 2. *Variation of S-D curve parameters with firing rate*

			S (ms) versus f_o (imp/s)			S_{max} (ms) versus f_o (imp/s)			Effective Interval (%) versus f_o (imp/s)		
			$S - k f_o^{-m}$			$S_{max} = k f_o^{-m}$			EI = $a f_o + b$		
	PP Amplitude, mV	Frequencies Examined, imp/s	k	m	R	k	m	R	a	b	R
Cell											
F1	0.5	17,* 18,* 20,* 25,* 33, 56, 63	44	1.5	0.89†	826	1.8	0.96†	−0.05	56	0.10
F1	0.9	17,* 20,* 25,* 33, 63	23	1.0	0.93	472	1.4	0.97†	−0.16	56	0.40
F2	0.8	11, 13.5, 14, 20, 25, 32	7.4	0.6	0.35	94	0.8	0.76	−1.4	77	0.77
F3	0.8	8,* 12, 14, 17, 20, 25, 33	20	0.9	0.93†	262	1.2	0.93†	0.0	51	0.00
F4	0.6	8.5,* 10,* 12.5,* 16.7, 25, 36	8.6	0.8	0.98†	46	0.9	0.84	1.5	54	0.88
F4	2.5	10,* 16.7, 24, 29	45	1.1	0.94	202	1.2	0.99	1.8	53	0.93
F5	0.8	12.5, 14, 16.7,* 25, 33, 45	29	1.0	0.96†	978	1.7	0.96†	1.1	46	0.85
F6	2.1	15,* 18.5,* 20,* 25	33	0.8	0.95†	653	1.4	0.98†	1.3	50	0.87
F7	0.4	13.3,* 21,* 25, 32, 45	4.8	0.7	0.81	151	1.2	0.80	0.4	65	0.30
F8	1.6	10,* 15, 17, 19, 25	86	0.9	0.46	111	0.5	0.38	1.1	62	0.50
F9	0.9	10,* 12.5,* 17.5, 24, 33	108	1.4	0.98†	840	1.7	0.98†	1.6	51	0.86
F10	3.6	10,* 12.5,* 17,* 20,* 24, 35, 49	127	0.9	0.99†	645	1.0	0.99†	0.69	62	0.88†
F11	0.8	21, 24, 33, 48	18	0.9	0.86	52	0.8	0.90	−0.16	89	0.17
F12	0.7	21, 25, 36, 40, 52, 71	[0.02f_o + 0.1‡]		0.63	[0.03f_o + 3.4‡]		0.33	0.21	64	0.77
Mean			42 ± 40	0.96 ± 0.25	85 ± 20	410 ± 340	1.2 ± 0.4	88 ± 17	0.57 ± 0.89	60 ± 12	0.59 ± 0.34

Values in Mean are ± SD. *Firing rates for which ISI lengthenings were observed. †Significance at $P < 0.01$ (2-tailed t test). ‡Values for linear regression. Mean ±SD were calculated for all cells, excluding values from *cell F12* for S and S_{max}. For abbreviations, see Table 1.
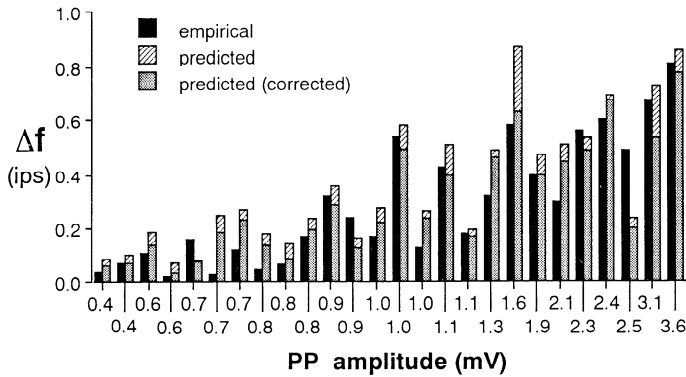
FIG. 7. Comparison between the Δf predicted from the shortening-delay (S-D) curve (striped bars) and the Δf empirically measured from the spike trains (solid bars). Gray bars show the predicted Δf corrected for interspike interval (ISI) lengthenings. Numbers on abscissa give amplitude of pulse potentials (PPs). These PPs were chosen for analysis because histograms showing the distribution of PPs in the ISI confirmed that the PPs appeared uniformly throughout the ISI.

cause the values of S calculated from the S-D curves ignored the lengthening of the subsequent ISIs; the match improved when the mean lengthenings were subtracted from the mean shortenings before calculation of Δf (gray bars). With the corrected S, Eq. 5 remains a good approximation to the Δf caused by the PPs.

Combining Eqs. 5 and 6A yields the following expression for the variation of Δf with PP amplitude for neurons firing at 25 imp/s

$$\Delta f = f_s * f_o * S(h)$$

$$= (f_s \text{ PP/s})(25 \text{ ips})(1.2 \ h^{1.24} \text{ ms/PP}) * (1 \text{ s}/10^3 \text{ ms}) \quad (5)$$

$$= 0.03 \ f_s h^{1.24} \text{ imp/s} \quad (8)$$

This also yields the average increment in firing caused by each PP: $\Delta \text{imp}/P = \Delta f/f_s = 0.03 \ h^{1.24} \text{ imp/PP}$. The plot of $\Delta \text{imp}/\text{PP}$ versus PP amplitude is shown in Fig. 3, A and B, and scaled on the right ordinate. With the use of linear regression, $\Delta \text{imp}/\text{PP}$ increased as 0.04 imp/PP/mV.

The fact that S varied inversely with firing rate (if we assume that $m = 1$ in Eq. 7) means that the change in firing rate caused by the PPs does not vary with the baseline firing rate. Combining Eqs. 5 and 7 and using a value of 1 for m yields

$$\Delta f = f_s f_o (k/f_o) = k * f_s \quad (9)$$

This was empirically confirmed by plotting Δf against baseline firing rate, as illustrated for one cell in Fig. 6D. Because slightly higher stimulus rates were used during rapid firing, the values were normalized by dividing by f_s. In 9 of 10 cells, Δf did not vary significantly ($P > 0.05$) with the baseline firing rate. In general, there was a good match between Δf and Δf_{emp}.

Because Δf does not vary significantly with firing rate, Eq. 8, which was obtained for cells firing at 25 imp/s, can be used to calculate Δf at any firing rate. Equating 8 with 9 yields the value of k as $0.03 \ h^{1.24}$.

Equation 9 predicts that Δf varies linearly with the stimulus rate. In one cell studied for a wide range of stimulus frequencies, Δf and Δf_{emp} appeared to increase linearly with the stimulus rate (Fig. 6E). The linear fit to Δf has a

slope of 0.13 ($R = 0.93$), which agrees well with the value of $k - 0.03 (3.6)^{1.24} = 0.15$.

Δf produced by transient versus steady current

Transient currents underlying the PPs can have a greater effect on firing rate than steady currents of the same average magnitude. The amount of firing produced by a steady current is documented by the frequency/current (f/I) curves. Figure 8A plots a portion of the steady-state f/I curve measured directly for one neuron. The slope of the line that best fits the data points (+) is ~ 22 imp/s/nA, comparable to the mean value of 22.4 imp/s/nA obtained for cat neocortical neurons by Stafstrom et al. (1984a). Superimposed on the plot are the calculated Δf caused by 1-ms current pulses introduced repetitively when the neuron was discharging at 25 imp/s (in response to a steady, 2.4-nA current). The pulses had amplitudes of 0.5 nA (0.4 mV), 1 nA (0.8 mV), and 4 nA (3.1 mV). With the use of Eq. 5 with $f_s = 25$ PP/s and values of S corrected for lengthening effects, these PP would produce net increases in firing rate of 0.4 ($\blacklozenge$), 0.8 ($\bullet$), and 4.9 imp/s ($\blacksquare$), respectively.

The vertical arrow in Fig. 8A shows the effective increase in firing rate for the largest PP. The changes in steady current (ΔI_{st}) needed to produce a comparable steady-state firing rate would be 0.22 nA, as indicated by the horizontal arrow from the data point to the f/I curve. In contrast, the PP introduced randomly into every ISI would represent an average current of 1 ms * 4 nA * 1 PP/40 ms = 0.10 nA.

Figure 8B plots the Δf produced by the PPs against their corresponding increases in average current. For comparison, the f/I curve is replotted on the same scale (dashed line). For a given increase in the average current, transient pulses clearly produce a greater increase than steadily applied current. For this cell, the PPs increased firing rate more effectively than steadily applied current by factors of ~ 1.5 (for the 400-μV PP) to 2.2 (for the 3.1-mV PP).

DISCUSSION

The aims of this study were 1) to investigate how the ISI shortenings caused by transient depolarizing potentials varied with their amplitude and the baseline firing rate, and 2) to derive an expression for the net increase in firing rate (Δf) caused by the depolarizing pulses. We found that the mean ISI shortening (S) increased with PP amplitude and was inversely proportional to the baseline firing rate of the neurons.

The Δf produced by PPs was proportional to stimulus frequency and increased with PP amplitude as a power function. A significant finding was that Δf did not vary with the baseline firing rate. Our results further suggest that fluctuations in the synaptic input can enhance the increases in the firing rate of neurons; transiently applied currents cause larger increases than an equivalent amount of steady current.

Variation of Δf with stimulus rate

The net increase in firing rate is proportional to the rate of PPs under the condition examined (stimulus rates $< \frac{1}{3}$ baseline firing rate). Calculation of Δf (Eq. 5) is restricted
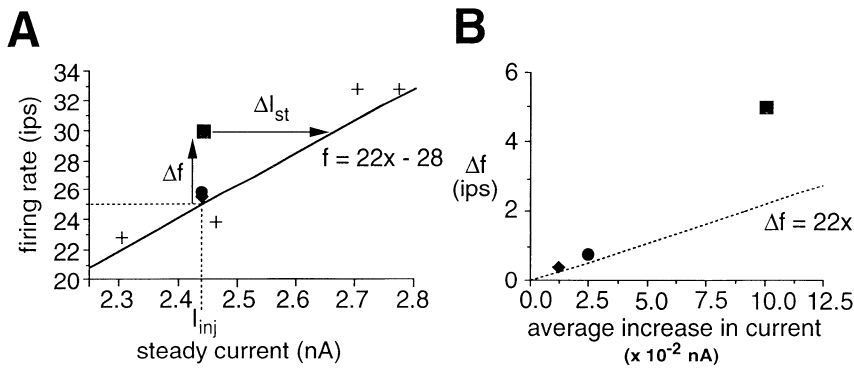
FIG. 8. Comparison of Δf produced by pulse potentials (PPs) with that produced by steady current injection. A: variation of steady-state firing rate with current injection; line represents linear portion of the frequency/current (f/I) plot ($f = 22x - 28$) for data points (+). Δf produced by 400 μV (diamond), 800 μV (triangle), and 3.1 mV PP (square) above a baseline firing rate of 25 imp/s are superimposed on the f/I plots (stimulus rate, 25/s). Horizontal arrow indicates increment in steady current (ΔI_{st}) needed to produce equivalent Δf as produced for large PP. B: Δf plotted against average current in the interspike interval. Symbols show the values for the 3 PPs above. Dotted line indicates the relation obtained with steady current injection.

to stimulus rates less than or equal to the baseline firing rate to avoid potential nonlinear summation of ISI shortenings caused by multiple PPs in the same ISI. The presence of two distinct processes, the slow regenerative process and the time-varying firing level (Reyes and Fetz 1993), may make the relation between ISI shortenings and multiple PPs nonlinear. Moreover, temporal summation of sufficiently rapid PPs could introduce a steady component to the stimulus waveform.

Variation of Δf with PP amplitude

The mean increase in firing rate was previously found to be directly proportional to EPSP amplitude in motoneurons and in models that have only the direct crossing mechanism (Fetz and Gustafsson 1983). In cortical neurons, the pooled data showed that the mean Δf varied with PP amplitude better as a power function than linearly (Fig. 3, A and B). The disproportionate effect of large PPs can be understood in terms of the two mechanisms by which the PPs can shorten the ISI. Small PPs shortened the ISI primarily by activating a slow regenerative process with a threshold below firing level (Reyes and Fetz 1993). Larger PPs caused significant ISI shortenings by crossing firing level directly for an increasing proportion of the ISI.

The large effective intervals were due to the fact that both the rising and decaying edges of the PPs triggered the slow regenerative process (Reyes and Fetz 1993). In addition, these neurons have a fast-activating, persistent sodium current that increases the amplitude and decreases the decay rate of the PP at depolarized levels (Reyes and Fetz 1993; Stafstrom et al. 1985; Thomson et al. 1988).

The lengthening of the ISI following the PP-shortened ISI further accentuates the difference in net Δf caused by large and small PPs. Although the ISI lengthening increased with amplitude (h) as a power function, the rate of increase ($h^{0.76}$) was significantly less than for the ISI shortening ($h^{1.24}$). Consequently, the interval lengthenings caused by the PPs were disproportionately greater for the smaller PPs than for the larger PPs. For example, the ISI lengthening would reduce the Δf caused by a 1-mV PP by $\sim$16%. In contrast, the lengthening would reduce the Δf caused by a 5-mV PP by only 7%.

Variation of Δf with baseline firing rate

The mean shortening, S, was inversely proportional to the baseline firing rate. This arose from the fact that the overall shape of the S-D curves, and hence the mean of the

S-D curves (%S), varied relatively little with firing rate. Because the S-D curve is normalized to the ISI, S (in ms) is a fixed proportion of the ISI (T_o); thus $S = (\%S/100)*T_o = constant*T_o = constant/f_o$. When this expression was inserted in Eq. 5, mean Δf varied only with the stimulus rate and PP amplitude (Eq. 8). Functionally, this implies that the Δf caused by PPs or EPSPs would not depend on the level of activity of the postsynaptic cell.

The overall shape of the S-D curve varied little with the baseline firing rate largely because the difference between the time-varying firing level and the membrane trajectory changed in proportion to the firing rate. Thus PPs were able to evoke direct crossings at the same relative delays in the ISI independently of the ISI duration. This shift in the time course of the firing level supports the hypothesis (Reyes and Fetz 1993) that the time-varying firing level was due to a decrease in the net inward current: the slow rise in the membrane trajectory at lower firing rates would allow more time for either an inward current to inactivate or an outward current to activate, thereby elevating the firing level.

The initial portion of the S-D curves exhibited a notable change at firing rates <25 imp/s. PPs that occurred early in the ISI often caused a paradoxical lengthening of the ISI. This lengthening may be related to the undershoot in the membrane trajectories caused by PPs occurring early in the ISI (Reyes and Fetz 1993). At a firing rate of $\geq$25 imp/s, the undershoot did not lengthen the ISI because it was followed immediately by a rapid rebound toward firing level. At lower rates, however, the rebound did not occur, and the ISI was lengthened (Reyes 1990). At 25 imp/s the undershoot may have decreased inactivation of the regenerative sodium current, causing the rebound. This may be absent for slower firing rates because the membrane trajectory approaches firing level slowly, allowing sufficient time for inactivation to redevelop.

Variation of Δf with the distribution of the PP in the ISI

Because the ISI shortening caused by the PP varied with its delay, Δf would also depend on the number of times the PP appeared at each delay in the ISI over many trials. For simplicity, the calculation of Δf assumed that the PP appeared uniformly throughout the ISI. Under this condition, S in Eq. 5 is the mean shortening calculated from the S-D curve. However, under certain conditions, the PP could appear preferentially at particular delays in the ISI. For example, the EPSPs from a collateral feedback circuit would tend to occur at a relatively fixed delay after a spike. Also, under

some conditions the firing of the pre- and postsynaptic cells may be sufficiently synchronized to generate preferential delays.

Depending on where in the ISI the PP preferentially appears, the Δf can vary significantly. For example, when the PP whose S-D curve is shown in Fig. 5B is introduced in each ISI of a cell firing at 12.5 imp/s, it will increase the firing rate by 6.3 imp/s if it preferentially appears at the delay producing the maximum shortening. If the PP appears with uniform probability throughout the ISI, the firing rate will increase by 1.6 imp/s. If it consistently appears at delay 15%, S will be negative, producing a paradoxical decrease in firing rate of ~0.9 imp/s.

Comparison of Δf caused by transients and by steadily applied current

Pyramidal cells discharge at a rate proportional to the amount of steady current that reaches the soma (Calvin and Sypert 1976; Koike et al. 1970; Stafstrom et al. 1984a). For sustained currents, the input-output transform is completely described by the steady-state f/I curve. Comparison of Δf produced by the PPs and Δf caused by the same average current applied steadily showed that the pulses produced a significantly greater increase in firing rate than would be predicted from the f/I curve. This difference is due to the fact that steadily applied current and brief transients have different effects on several ionic conductances. In neocortical neurons, adaptation of firing rate in response to steadily injected current appears to result from a decrease in the net inward current, because of the activation of several potassium conductances (Schwindt et al. 1988b,c) and the deactivation of the anomalous rectifier (Schwindt et al. 1988a; Spain et al. 1987). Both effects have relatively long time constants (>50 ms for activation of the potassium conductances and >35 ms for deactivation of the anomalous rectifier) and are therefore much less influenced by brief PPs than by sustained stimuli. In contrast, the conductances that the PPs could affect significantly in the subthreshold range include the fast-activating persistent sodium current, which has been shown to increase the amplitude of EPSPs (Deisz et al. 1991; Stafstrom et al. 1985; Thomson et al. 1988), and could enhance the PPs' ability to shorten the ISI.

Variation of Δf with the time course of the synaptic current

Because voltage transients produce a greater Δf than the same net current applied steadily, the effect of a population of presynaptic neurons can depend significantly on correlations in their discharge patterns. A large population of presynaptic cells whose activities are completely uncorrelated would produce a predominantly steady synaptic current because their randomly occurring unitary inputs are evenly distributed over time. On the other hand, if the same cells fire synchronously, they could produce relatively large voltage transients. The following calculation illustrates the effects of changing the synchrony of presynaptic units on the firing rate of a postsynaptic neuron.

Assume that 1) the postsynaptic neuron is firing repetitively owing to a steady background input; and 2) each presynaptic unit is firing repetitively at a rate f_i. The net
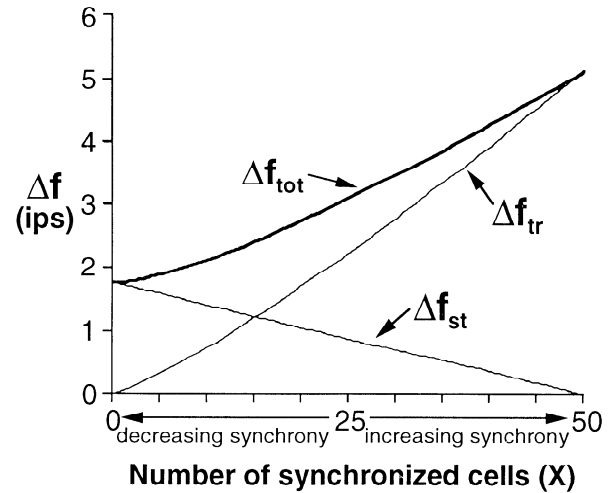
FIG. 9. Variation of Δf as a function of synchrony in the firing of 50 presynaptic neurons (with constant net synaptic current). Abscissa represents the number of synchronized cells. Δf_{st} is the predicted Δf produced by the component of steadily applied current; the values were calculated from a frequency/current plot with a slope of 22.4 imp/s/nA. Δf_{tr} is the predicted Δf produced by transients as calculated by Eq. 8. Δf_{tot} is the sum of Δf_{st} and Δf_{tr}.

synaptic current can be considered to consist of a steady component, I_{st}, and a transient component, I_{tr}. The total change in firing rate, Δf_{tot}, above a baseline firing rate is the sum of the Δf due to the steady component, Δf_{st}, and the transient component, Δf_{tr}

$$\Delta f_{tot} = \Delta f_{st} + \Delta f_{tr} \qquad (10)$$

Δf_{st} can be estimated from the product of ΔI_{st} and the slope of the f/I curve, $k_{f/I}$.

$$\Delta f_{st} = k_{f/I} * \Delta I_{st} \qquad (11)$$

In the limiting case, a predominantly steady current can be generated by the completely asynchronous activity of many units. The number of units (m) is assumed to be large enough to generate negligible ripple compared with the level of steady current. If the unitary current pulses from the neurons have width w and amplitude I_i

$$\Delta I_{st} = m * f_i * I_i * w \quad (nA) \qquad (12)$$

If x of these units fire in synchrony, their unitary currents summate to produce a large transient current that can be estimated by

$$I_{tr} = x * I_i \qquad (13)$$

I_{tr} will occur at a rate equal to the units' firing rate, f_i. Modeling the cell membrane as a resistor and capacitor in parallel, the height, h, of the EPSP is approximately

$$h = I_{tr} * R_n * (1 - e^{-w/\tau_m}) \qquad (14)$$

where R_n is the input resistance (taken to be 11.7 MΩ) (Stafstrom et al. 1984b) and τ_m is the membrane time constant (taken to be 6.9 ms) (Stafstrom et al. 1984b).

Figure 9 illustrates Δf_{tot} generated by the activities of 50 presynaptic units as a function of their synchrony. Each unit fires at 25 imp/s and causes a rectangular synaptic current with an amplitude of 0.063 nA and width of 1 ms (producing a 100-μV EPSP). When the inputs are completely asynchronous, the 50 units firing at 25 imp/s will generate a predominantly steady current of 0.08 nA, which

will increase the firing rate by $\sim$1.8 imp/s [taking the slope of the f/I curve to be 22.4 imp/s/nA (Stafstrom et al. 1984a)]. As the proportion of synchronous units is increased, Δf_{st} decreases while both Δf_{tr} and Δf_{tot} increase. When all the units fire synchronously, Δf_{tot} reaches a maximum value. At this extreme, the units generate a compound EPSP with an amplitude of 5 mV, which will increase the firing rate by $\sim$5.1 Hz. Thus the same number of neurons will produce a threefold greater increase in firing rate when they fire synchronously. The enhancing effect of synchrony has been confirmed for simulations with a neuron model incorporating three conductances (Murthy and Fetz 1993).

Functional significance

The firing rate of neocortical neurons may be increased by two distinguishable changes in synaptic input. First, the level of steady synaptic input may be increased by increasing the number or the firing rate of asynchronously active units. Second, the magnitude of voltage transients may be increased through synchronization of already active units or through recruitment of afferents that produce large EPSPs. The present results suggest that the latter mechanism could play an important role in neuronal communication, for several reasons.

First, because voltage transients are more effective in increasing the firing rate, fewer synchronously active presynaptic units would be needed to produce a given increase in firing rate (Figs. 8 and 9). Second, transients are more effective in sustaining high discharge rates for prolonged periods of time. In the in vitro slice preparation we found that many pyramidal cells are unable to maintain discharge rates of >50 imp/s for prolonged times in response to steady current injection. The spikes widened and shortened until the cells stopped firing; the elevated potential associated with high discharge rates probably inactivated the regenerative sodium current. To the extent that transients do not produce sustained depolarizations, they may avoid such inactivation.

Third, large transients may also be important for synchronizing the firing of many cells. Because the direct crossings occurred on the rising edge of the large EPSPs, the evoked spikes occur within a relatively short latency after the onset of the EPSP. Thus large compound EPSPs arriving together in postsynaptic cells would cause them to fire in synchrony. In turn, these synchronously activated neurons would tend to produce large EPSPs, thereby synchronizing the firing of their target neurons.

Recent observations of coherent oscillations in cortical field potentials and unit activity (Eckhorn et al. 1988; Gray et al. 1989; Murthy and Fetz 1992) raise the possibility that large transient depolarizations may be used by the nervous system to mediate functions beyond simple rate coding of behavioral parameters. These potentials appear in phase over large cortical regions under certain behavioral conditions, suggesting synchronous activation of dispersed populations of neurons. These oscillatory potentials are associated with large depolarizing transients in cortical neurons (Chen and Fetz 1991; Jagadeesh et al. 1992). Thus, in contrast to the cells' rate coding properties, such synchronous

depolarizations may facilitate synaptic interactions between large populations of neurons involved in common perceptual or attentional mechanisms.

REFERENCES

ABELES, M. *Corticonics: Neural Circuits of the Cerebral Cortex.* Cambridge, UK: Cambridge Univ. Press, 1991.

CALVIN, W. H. AND SYPERT, G. W. Fast and slow pyramidal tract neurons: an intracellular analysis of their contrasting repetitive firing properties in the cat. *J. Neurophysiol.* 39: 420–434, 1976.

CHEN, D. F. AND FETZ, E. E. Intracellular correlates of oscillatory activity of cortical neurons in awake behaving monkeys. *Soc. Neurosci. Abstr.* 17: 310, 1991.

CREUTZFELDT, O. D., KUHNT, U., AND BENEVENTO, L. A. An intracellular analysis of visual cortical neurones to moving stimuli: responses in a co-operative neuronal network. *Exp. Brain Res.* 21: 251–274, 1974.

DEISZ, R. A., FORTIN, G., AND ZIEGLGÄNSBERGER, W. Voltage dependence of excitatory postsynaptic potentials of rat neocortical neurons. *J. Neurophysiol.* 65: 371–382, 1991.

DOUGLAS, R. J. AND MARTIN, K. A. C. Neocortex. In: *The Synaptic Organization of the Brain* (3rd ed.), edited by G. M. Shepherd. Oxford, UK: Oxford Univ. Press, 1990, p. 389–438.

ECKHORN, R., BAUER, R., JORDAN, W., BROSCH, M., KRUSE, W., MUNK, M., AND REITBOECK, H. J. Coherent oscillations: a mechanism of feature linking in the visual cortex? *Biol. Cybern.* 60: 121–130, 1988.

FERSTER, D. Orientation selectivity of synaptic potentials in neurons of cat primary visual cortex. *J. Neurosci.* 6: 1284–1301, 1986.

FETZ, E. E. AND GUSTAFSSON, B. Relation between shapes of postsynaptic potentials and changes in firing probability of cat motoneurones. *J. Physiol. Lond.* 341: 387–410, 1983.

GRAY, C. M., KONIG, P., ENGEL, A. K., AND SINGER, W. Oscillatory responses in cat visual cortex exhibit inter-columnar synchronization which reflects global stimulus properties. *Nature Lond.* 338: 334–337, 1989.

JAGADEESH, B., GRAY, C. M., AND FERSTER, D. Visually evoked oscillations of membrane potential in cells of visual cortex. *Science Wash. DC* 257: 552–554, 1992.

KOIKE, H., MANO, N., OKADA, Y., AND OSHIMA, T. Repetitive impulses generated in fast and slow pyramidal tract cells by intracellularly applied current steps. *Exp. Brain Res.* 11: 263–281, 1970.

MATSUMURA, M. Intracellular synaptic potentials of primate motor cortex neurons during voluntary movement. *Brain Res.* 163: 33–48, 1979.

MURTHY, V. N. AND FETZ, E. E. Coherent 25- to 35-Hz oscillations in the sensorimotor cortex of awake behaving monkeys. *Proc. Natl. Acad. Sci. USA* 89: 5670–5674, 1992.

MURTHY, V. N. AND FETZ, E. E. Effects of input synchrony on a model neuron. In: *Computational and Neural Systems,* edited by F. Eekman and J. Bower. New York: Kluver Academic. In press.

REYES, A. D. *Effects of Brief Depolarizing Pulses on the Firing Rate of Cat Neocortical Neurons* (PhD thesis). Seattle, WA: Univ. of Washington, 1990.

REYES, A. D. AND FETZ, E. E. Two modes of interspike interval shortening by brief transient depolarizations in cat neocortical neurons. *J. Neurophysiol.* 69: 1660–1671, 1993.

SCHWINDT, P. C., SPAIN, W. J., AND CRILL, W. E. Influence of anomalous rectifier activation on afterhyperpolarization of neurons from cat sensorimotor cortex in vitro. *J. Neurophysiol.* 49: 468–481, 1988a.

SCHWINDT, P. C., SPAIN, W. J., FOEHRING, R. C., CHUBB, M. C., AND CRILL, W. E. Slow conductances in neurons from cat sensorimotor cortex in vitro and their role in slow excitability changes. *J. Neurophysiol.* 59: 450–467, 1988b.

SCHWINDT, P. C., SPAIN, W. J., FOEHRING, R. C., STAFSTROM, C. E.,

CHUBB, M. C., AND CRILL, W. E. Slow conductances in neurons from cat sensorimotor cortex in vitro and their role in slow excitability changes. *J. Neurophysiol.* 59: 424–449, 1988c.

SPAIN, W. J., SCHWINDT, P. C., AND CRILL, W. E. Anomalous rectification in neurons from cat sensorimotor cortex in vitro. *J. Neurophysiol.* 57: 1555–1576, 1987.

STAFSTROM, C. E., SCHWINDT, P. C., CHUBB, M. C., AND CRILL, W. E. Properties of persistent sodium conductance and calcium conductance of layer V neurons from cat sensorimotor cortex in vitro. *J. Neurophysiol.* 53: 153–169, 1985.

STAFSTROM, C. E., SCHWINDT, P. C., AND CRILL, W. E. Repetitive firing in layer V neurons from cat neocortex in vitro. *J. Neurophysiol.* 52: 264–277, 1984a.

STAFSTROM, C. E., SCHWINDT, P. C., AND CRILL, W. E. Cable properties of layer V neurons from cat sensorimotor cortex in vitro. *J. Neurophysiol.* 52: 278–289, 1984b.

THOMSON, A. M., GIRDLESTONE, D., AND WEST, D. C. Voltage-dependent currents prolong single-axon postsynaptic potentials in layer III pyramidal neurons in cat neocortical slices. *J. Neurophysiol.* 60: 1896–1907, 1988.